Effect of Heating Rate on the Recrystallization Behaviour of Doped Tungsten

O. Horacsek[1], C.L. Briant[2] and K. Horacsek[1]

[1]*Research Institute for Technical Physics of the Hungarian Academy of Sciences*
H-1325 Budapest, P.O. Box 76, Hungary
[2]*General Electric Corporate Research and Development*
1 River Road, Schenectady, NY 12345, USA

ABSTRACT

The influence of heating rate on the development of primary and secondary recrystallized grain structure of heavily drawn KSiAl-doped tungsten wires has been studied by using TEM, SEM, EEM and microhardness measurements. The observed difference in the microstructures between the rapidly and slowly heated wires is discussed in terms of the interaction between grain boundaries and bubbles. It is suggested that on slow heating, the boundaries of the widening fibers can move slowly enough to drag along partial or entire bubble rows. As a result of the collective motion of bubbles and boundaries, longer "secondary" bubble barriers can form from the shorter original "primary" ones, thereby contributing to the evolution of the recrystallized grains with high aspect ratio. From microhardness measurements and from the results of EEM experiments, it is also concluded that slow heating decreases the driving force for secondary recrystallization requiring a higher temperature at which the enhanced grain boundary mobility results in a large grained structure of the wire.

I. INTRODUCTION

Theoretical consideration of the interaction between dislocations and second phase particles indicated that at high temperatures and low stresses, elastically soft particles, such as liquid or gaseous bubbles, are more effective in blocking the motion of dislocations than hard particles /1,2/. Consequently, strengthening against dislocation creep can be achieved by a bubble forming dopant material that must be highly insoluble in the matrix, otherwise diffusional Ostwald ripening between the bubbles of different sizes would reduce the dispersion strengthening effect and would produce large bubbles for creep voids. In incandescent lamps, where tungsten filaments experience high temperatures and low gravitational stresses, the wire is strengthened by potassium bubbles having diameters of the order of 10 nm /3/. The potassium is introduced into the tungsten by a powder metallurgy technique involving KSiAl-doping of the oxide, its reduction to metal powder and compacting to ingots /4-7/. During high temperature sintering of the ingot, the K, Si, and Al containing dopant particles decompose and most of the silicon and aluminium are removed, while the insoluble and, hence, non-diffusing potassium remains entrapped in the residual pores of the ingot. When the sintered ingot is processed by swaging and wire drawing, the potassium pores are elongated in the working direction into narrow ellipsoids and on annealing each potassium ellipsoid breaks up into a single row of spherical bubbles /8-11/.

As the temperature of the wire is increased, two distinct stages occur: a relatively uniform structural coarsening (usually called primary recrystallization), followed by exaggerated grain growth which is mostly referred to in the literature on KSiAl-doped tungsten as secondary recrystallization, although the usage of this term is questionable /12-16/. During recrystallization, the bubble rows act as barriers against grain boundary migration, and long grains with interlocking boundaries are formed that make grain boundary sliding difficult. Thus, the potassium bubbles in KSiAl-doped

tungsten wires exert their strengthening effect not only directly by pinning dislocations /1/, but also indirectly by promoting the formation of a highly elongated, overlapping recrystallized grain structure. Previous studies have shown that both bubble distribution /17/ and the rate at which recrystallization occurs /18,19/ have a marked effect on the grain morphology and, hence, on the mechanical properties of the wire. In this paper we present some observations on the effect of heating rate on the formation of primary and secondary recrystallized grain structures of KSiAl-doped tungsten wires. For this study two considerably different heat treatments were applied for the same material. The purpose of this work was to study the changes in the bubble dispersion and grain morphology as a function of the annealing conditions in order to understand the effect of heating rate on the recrystallization process of doped (bubble strengthened) tungsten wires.

II. EXPERIMENTAL METHODS

All samples used in this study stemmed from the same spool of as-drawn wire that was processed from a KSiAl-doped sintered ingot. The ingot with 17.2 g/cm^3 sintered density and 74 wt ppm potassium content was swaged and drawn to a diameter of 0.39 mm at progressively decreasing temperatures, according to a proprietary process. The wire samples were annealed by self resistance heating in vacuum at pressures below 10^{-3} Pa. Two different rates of heating were applied. In the case of rapid heating, the temperature of the wire was increased within 10 seconds from room temperature to 1800°C and then held at this temperature for 5 minutes. In the case of slow heating, the temperature was increased linearly over 30 minutes to 1800°C followed by an isothermal hold for 5 minutes.

The primary recrystallized grain structures (coarsened fiber structures) after heat treatments at 1800°C were examined on the longitudinally fractured surfaces by scanning electron microscopy (SEM). After exaggerated grain growth (secondary recrystallization), the microstructure was investigated on the longitudinally sectioned and polished surfaces by optical microscopy. The primary recrystallized grain structure was characterized by histograms for the widths and lengths of the grains of the rapidly and slowly heated samples.

These plots were obtained after more than 400 grains had been counted. The grain aspect ratio (ratio of the length and width of the grains) was used for both the fine grained primary structure (l/w) and for the large grains formed during secondary recrystallization (L/W). While the lengths and the widths of the primary grains were separately measured on the SEM micrographs, and thus, l/w was calculated from the obtained averages, the aspect ratios of the large secondary grains that formed during exaggerated grain growth, L/W, were directly estimated on the optical micrographs.

The bubble dispersion of the samples was quantitatively characterized by histograms of the size distribution of the potassium bubbles using thin foil transmission electron microscopy (TEM). In order to compare the bubble structure of the rapidly heated wires with that of the slowly annealed counterparts, a number of TEM micrographs, taken from randomly chosen areas, were evaluated. For the size distribution histograms, the diameters of more than 500 bubbles were measured in both cases. Since SEM allowed detection on the intergranular fracture surfaces of only the large bubbles, to get more information about the intergranular bubble population, additional TEM examinations using thin foil fractographic replication techniques were conducted. For these investigations single-stage Pt/C replicas were taken from the fractured surfaces.

Kinetic studies of the secondary recrystallization were performed using emission electron microscopy (EEM). The temperature of the sample in the EEM was increased by self-resistance heating and the temperature was measured by an optical pyrometer. The orientation contrast of the electron optical pictures allowed the temperature at which secondary recrystallization started to be measured and the details of the recrystallization process to be observed by watching the migration of the grain boundaries on the EEM screen /19,20/. Video tape recordings from the process were evaluated during playback at a lower speed. The progress of secondary recrystallization of the doped wire was determined by

measuring the time dependence of the volume fraction of the recrystallized material.

To analyze the role of the stored deformation energy on the kinetics of recrystallization, microhardness measurements were made on a range of annealed samples. By means of these measurements we attempted to follow the changes in the stored energy as a function of time during isothermal annealing of the wire at a temperature near to the onset of secondary recrystallization. The hardness was measured with a Reichert microhardness tester under a load of 100 g. The average hardness values were determined on the basis of 40 measurements for each annealing time.

III. RESULTS

Effect of Heating Rate on Recrystallized Microstructure

Typical SEM micrographs from longitudinally fractured surfaces showing the fiber structure of the as-received wire as well as the primary grain structures of the rapidly and slowly heated samples are given in Figure 1. Quantitative evaluation of the grain structures for the two differently annealed wires are shown in Figure 2 and Figure 3 representing the distribution of lengths (l) and widths (w) of the primary grains formed in the rapidly and slowly heated samples. The histograms show that the slow heating rate generated longer primary grains, while the influence on the widths of the grains was less pronounced; only a slight widening was detected. EEM experiments indicated that after slow heating, secondary recrystallization started consistently at higher temperatures. Microstructural examination showed that after exaggerated grain growth, the aspect ratio of the large secondary grains, L/W, was greater than the grain aspect ratio in the rapidly heated counterparts. The results are summarized in Table I showing that l/w and L/W are related values: the greater the aspect ratio of the primary grains, the greater the aspect ratio of the large secondary grains in the final structure (Fig. 4).

TEM revealed the characteristic bubble rows in all samples. In agreement with previous studies /21/, we also found that, as a result of the irregular distribution of the bubble rows, the samples contained bubble rows situated very close to each other and, hence, in some places the distance between the neighbouring rows was comparable to or even less than the spacing between the individual bubbles in a row, as shown in Figure 5. The size distributions of the bubbles in the rapidly and slowly heated wires are shown in Figure 6. The difference between the two histograms (the appearance of a bubble population in the 70-120 nm size range in the slowly heated wire) reflects the fact that the slow wire heating allowed a noticeable bubble coarsening. The larger percentage of the bubbles in the 0-10 nm range in Figure 6(b) is probably due to the relatively large error in the size determination for the smallest bubbles: while some bubbles in the rapidly heated wire were not counted because they were too small, after coarsening, the larger bubbles in the slowly heated wire were more perceptible and they could be counted reliably.

EEM Observations on Kinetics of Secondary Grain Growth

Although the temperature at which secondary recrystallization in doped tungsten starts depends not only on the wire history, but also on the heating rate /19/, in agreement with previous studies /22/, our direct observations by EEM showed that a minimum temperature must be exceeded for secondary grain growth. The lowest temperature at which secondary recrystallization began was detected on the screen for different heating rates. In the case of the examined KSiAl-doped material no secondary recrystallization could be observed below 1800°C. Therefore, in our EEM studies, the wire was first brought to 1900°C in 2 seconds (the sample was flashed) and then the recrystallized fraction of the sample was recorded as a function of time and temperature. Although at 1900°C secondary recrystallization began, after initial rapid grain growth the moving boundaries were usually blocked in their motion and further grain growth did not occur even after prolonged heating. (At higher temperatures, for example at 2000°C, essentially similar behaviour was observed: after a short period of grain growth, boundary migration stopped and a part of

a)

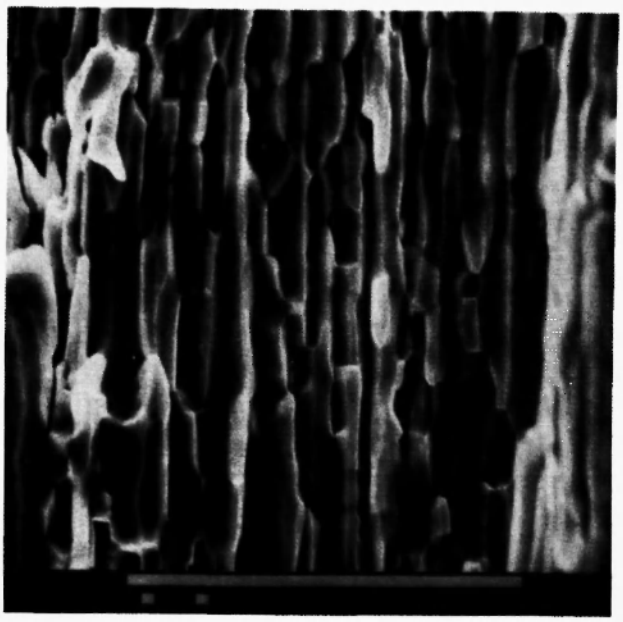

b)

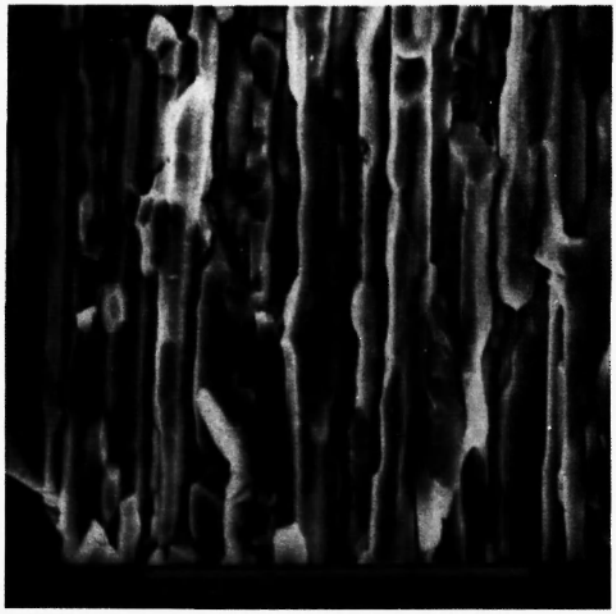

c)

Fig. 1: SEM micrographs of longitudinally fractured surfaces of as-received wire (a), and the primary recrystallized structure of rapidly heated (b) and slowly heated (c) samples. The micron marker represents 10 μm.

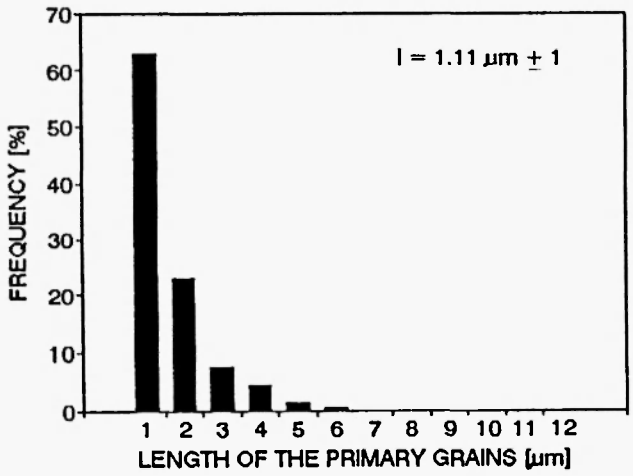

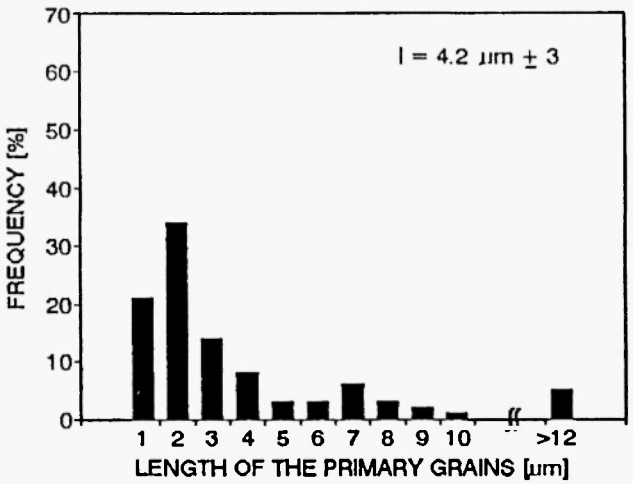

Fig. 2: Histograms showing the lengths of the primary grains after rapid (a) and slow (b) heating.

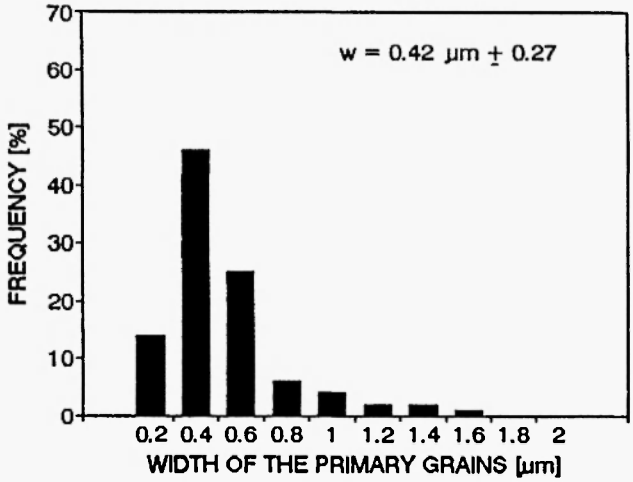

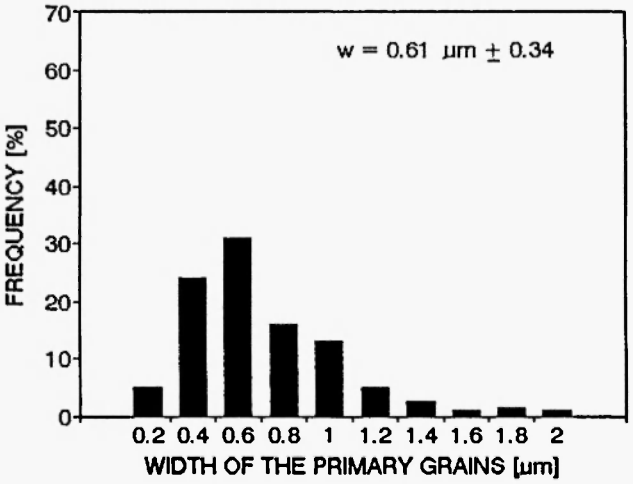

Fig. 3: Histograms showing the widths of the primary grains after rapid (a) and slow (b) heating.

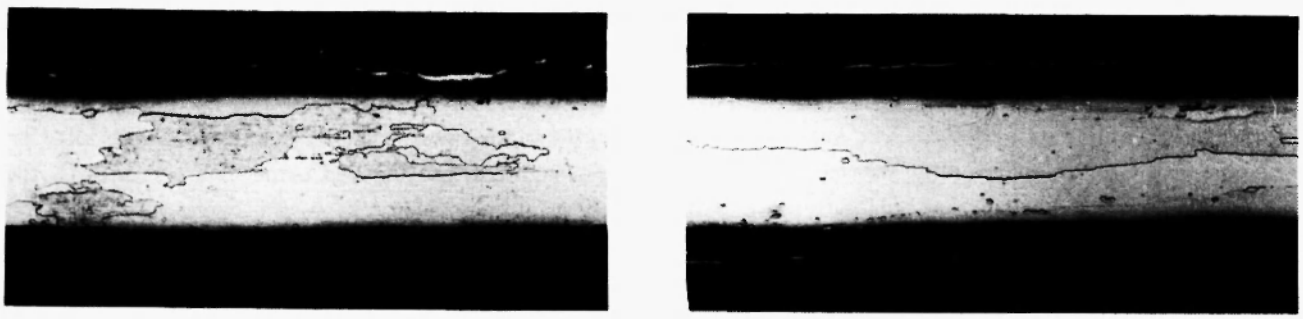

Fig. 4: Secondary grain structures after rapid (a) and slow (b) heating.

Fig. 5: TEM micrograph showing bubble rows situated close to each other.

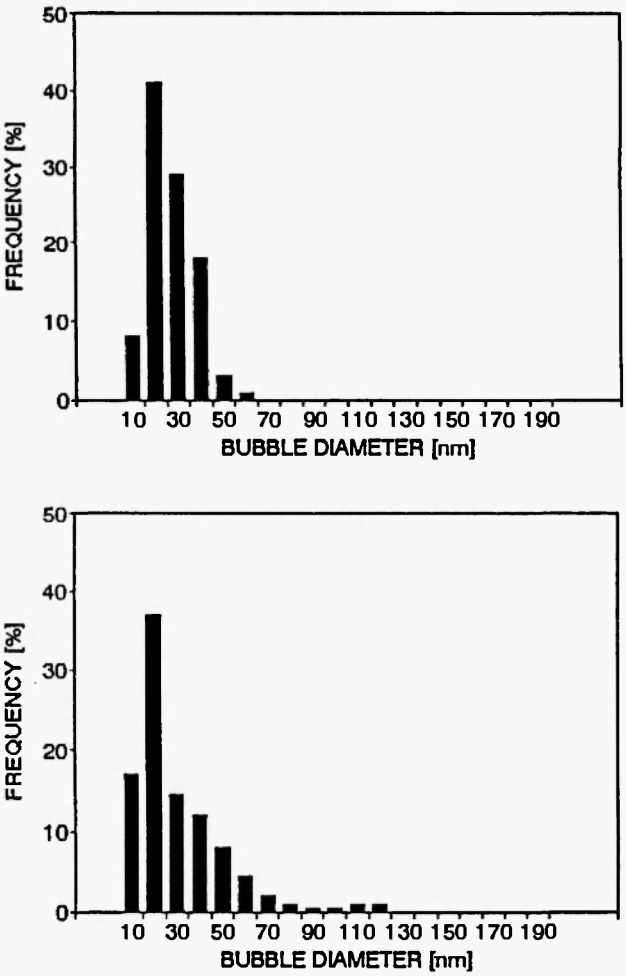

Fig. 6: Distribution of bubble diameters after rapid (a) and slow (b) heating.

the sample remained unrecrystallized at the given temperature.)

We observed that whenever grain growth was arrested and subsequently the wire was further heated for a long time (e.g. 20 minutes) the recrystallization process could not be completed at the given temperature. In this case continuation of the blocked recrystallization process (further movement of grain boundaries) required a considerable increase in the temperature. A typical kinetic plot is given in Figure 7(a) showing that as the temperature of the wire was raised to 1900°C, a part of the sample (~30%) was occupied within 3 seconds by a large growing grain, and subsequently no (or only some occasional) grain boundary movements could be observed. If this partly recrystallized sample was further heated at 1900°C for 20 minutes, we had to increase the temperature to 2300°C, in order to attain full recrystallization. In these experiments we went up in 100°C increments and after a 1 minute hold the recrystallized fraction of the sample was recorded. Figure 7(a) shows that no response was found for the applied three 100°C increments, and further grain growth could be attained only at 2300°C.

In contrast, only a relatively small increase in the temperature was required for the continuation of the arrested secondary recrystallization if the temperature of the sample was raised within a few seconds after the grain growth process had come to a standstill. If the recrystallization process again came to a stop, an immediately applied slight rise (~20°C) of the temperature proved to be sufficient to produce further grain growth. Figure 7(b) shows that in this way (annealing at progressively increasing temperatures) complete recrystallization was reached in the same

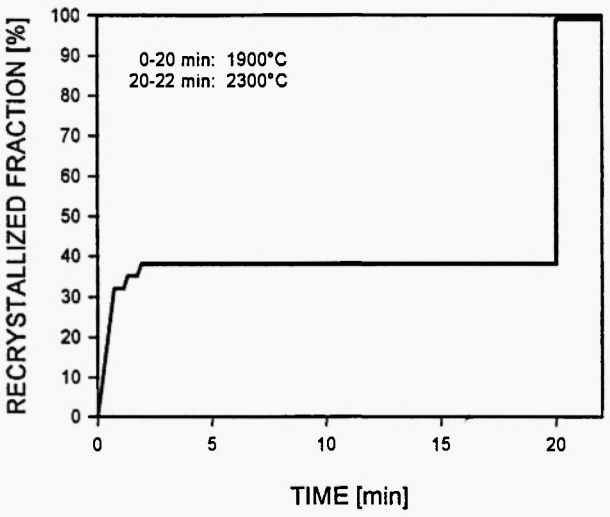

Fig. 7(a): Typical kinetic plot showing that after prolonged heating of the partly recrystallized wire, a considerable increase in the temperature is required for continuation and completion of the arrested recrystallization.

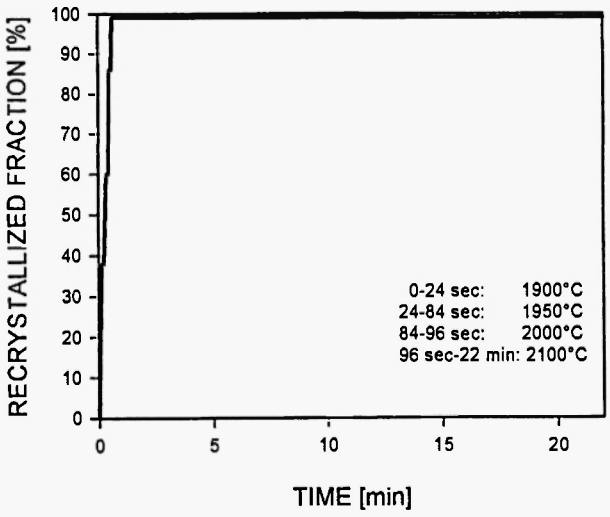

Fig. 7(b): Typical kinetic plot showing that complete recrystallization can be attained at a lower temperature if a quick heat up is applied.

material at about 200°C lower temperature compared with the above described annealing treatment (Figure 7(a)), when the partly recrystallized wire was heated at the given temperature for a relatively long time. Thus, depending on the heating conditions, a considerable difference was measured in the lowest temperature to which we had to raise the temperature of the wire to obtain full recrystallization.

Measurements to Follow the Release of Stored Deformation Energy

Figure 8 shows the changes in hardness with time at 1800°C. In the case of these measurements the wire was flashed to 1800°C and then held at this temperature for different times. As a basis for comparison, the hardness of the as-received wire is also indicated. Although the error bars are relatively large, the plot demonstrates that after a sharp drop (measured after 10 seconds), a further decrease in hardness occurred with time for about 20 minutes. We also made additional measurements on the interrupted anneal samples to record the widening of the fibers as a function of time during isothermal annealing at the same temperature (1800°C). The results given in Figure 9 show that the microhardness decreased in the same manner as the primary grains increased in width during the anneal until finally a limiting "saturation" value of 0.78 ± 0.08 μm was reached.

IV. DISCUSSION

Figures 1-3 and Table I show that the applied slow heating rate resulted in an increased length of the primary grains. If one takes into consideration that one of the primary factors controlling the evaluation of the primary grain structure is the rows of potassium-containing bubbles, we can suggest that the development of the longer primary grains in the slowly heated samples is a manifestation of the effect of longer longitudinal bubble barriers. If this idea is correct, then the slowly heated samples should have longer bubble rows. A comparison of the two bubble size distribution histograms in Figure 6 also indicates that during slow heating of the wire some bubble coarsening occurred. It does not seem likely that this difference can be simply explained by bubble growth resulting from the internal pressure of the potassium gas.

The experimentally observed differences between

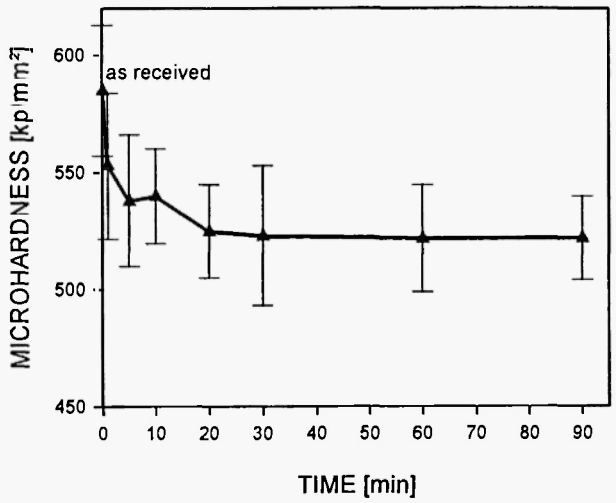

Fig. 8: Changes in microhardness with time during isothermal annealing at 1800°C.

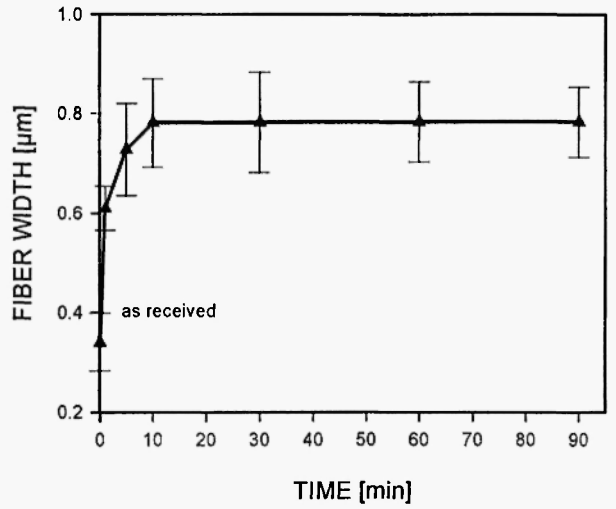

Fig. 9: Widths of the primary grains vs annealing time at 1800°C.

the slowly and rapidly heated wires are the following:

a) The lengths of the primary grains were longer in the slowly heated wire;
b) The size distribution of the bubbles showed that there were large bubbles present in the slowly heated wire.

These could be explained in the following way. A fiber boundary which is subjected to a driving force for recrystallization exerts a force (pull) on the bubbles that are located in the boundary. This force per bubble is derived from the energy that must be supplied in order to separate the bubble from the boundary /23/. On the basis of this consideration one obtains for the maximum critical attractive force $F_c = 2\gamma r\pi$ and the pinning force (Zener drag) exerted on a moving grain boundary by the bubbles is given by /24/

$$F_p = 2\pi r\gamma Z \qquad (1)$$

where r is the radius of the bubbles, Z is the number of bubbles intersected by a unit of the boundary and γ is the grain boundary energy per unit area.

On the other hand, as a result of the mechanical deformation, dislocations and fiber boundaries are created in the wire. This stored deformation energy provides a driving force for recrystallization that may be estimated from the dislocation and boundary energies as

$$F_d = NGb^2 + \frac{3\gamma}{D} \qquad (2)$$

Table I

Data showing the effect of heating rate on the grain aspect ratios of primary (l/w) and secondary (L/W) grains and on the onset of secondary recrystallization

heating rate	fiber lengths l [µm]	fiber widths w [µm]	l/w	L/W	onset of secondary recrystallization [°C]
rapid	1.11 ± 1	0.42 ± 0.27	2.6	8 ± 4	1900
slow	4.2 ± 3	0.61 ± 0.34	6.9	26 ± 17	2200

where N is the dislocation density, G is the shear modulus, b is the Burgers vector and D is the grain diameter. Although in the case of drawn tungsten wire it is difficult to make exact calculations (e.g. both in the as-drawn and primary recrystallized conditions the grain shape is far from equiaxed), estimates from expressions (1) and (2) have shown that the average driving and pinning forces in doped tungsten wires do not differ significantly /15,24,25/. Thus, the progress of recrystallization is governed by local fluctuations in the driving and pinning forces.

The spatial distribution and length of the latent bubble rows (i.e. the arrangement and dimension of the elongated potassium ellipsoids) in the as-drawn wire is determined by the process history /11,26,27/. If the observed difference in the aspect ratio of the primary grains is a result of having longer bubble rows in the slowly heated sample, these bubble rows must be created in some way during the heating. Therefore, we must have a mechanism by which the original rows can gather together along the longitudinal grain (fiber) boundaries to form the longer bubble rows (longer barriers against grain boundary movement).

Figure 6 shows that during slow wire heating bubble coarsening occurred. Taking into consideration that potassium is insoluble in tungsten and, hence, the solubility of the bubbles is practically zero, bodily migration of the bubbles and subsequent coalescence seems to be the only mechanism by which the bubbles can coarsen. On rapid heating, the migration of the fiber boundaries is driven by a sudden release of a large stored energy and detachment may occur readily from the bubbles. Therefore the initial bubble distribution is not considerably modified by boundary movement. On slow heating, however, the bubbles could remain attached to the boundaries of the widening fibers which could move slowly enough to drag along the bubbles. In this case the velocity of the boundary migration is controlled by the movement of bubbles that are attached to the boundary /28-30/. As the fibers broaden, partial or even entire bubble rows could be dragged by the boundary segments moving in the transverse direction. As a result of row-row collisions, bubble coalescence and long bubble rows could form from the joined bubble rows, as illustrated schematically in Figure 10.

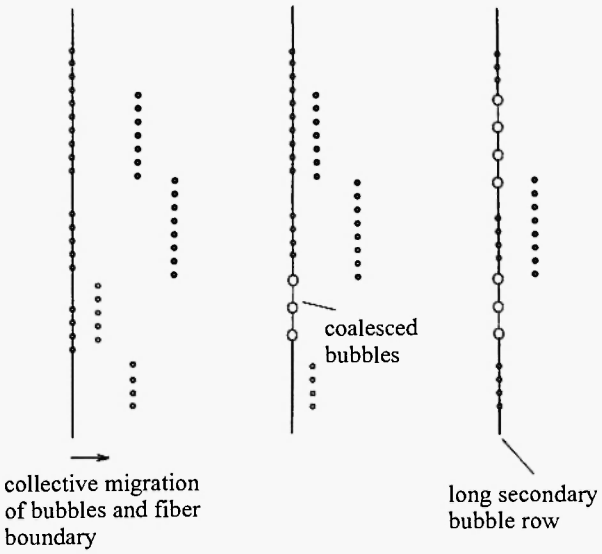

Fig. 10: Schematic illustration of the formation of long "secondary" bubble rows.

Our interpretation of the evolution of long primary grains seems to be consistent with the results of fracture replication TEM experiments. Figure 11 shows that the longitudinal boundaries of the primary grains in the *slowly heated wire contained long bubble rows which consisted of bubbles of different sizes with different spacings between them.* Since the sintered ingot has a wide variety of pore sizes, the bubble formation theory of Moon and Koo /8/ predicts that *the length of the bubble rows might be very different, but the size of the bubbles and the spacing between them must be identical for a given bubble row* /31/. Thus, we would expect a bubble row produced by the break-up of a single potassium ellipsoid to contain bubbles of identical sizes and spacings. The discrepancy between the theory and experimental facts (variable sizes and spacings within a single bubble row) can be explained by the mechanism as shown in Figure 10.

While the spacing between the bubbles in a given row is, in principle, determined by the size of these bubbles /8,27/ (it should be a few times larger than their diameters), there is no theoretical limitation on the distance between the rows. As a result of the wide variety in the spatial distribution of the potassium pores in the sintered ingot, the distance by which the bubble rows are separated from each other in the wire varies

quite a lot and, hence, it may also be very small as shown in Figure 5. At such places collision and coalescence of bubbles of adjacent rows requires only a slight displacement of the laterally moving fiber boundary by which the bubbles are dragged through the matrix to the neighbouring bubble row. Since row-row collision results in a new bubble row (Fig. 10), depending on the distribution of the potassium ellipsoids in the as-drawn wire, and on the annealing conditions, more or less relatively long "secondary" bubble row can form from the original "primary" ones contributing to the development of higher aspect ratios of the recrystallized grains. The observed microstructural response to the annealing treatment indicates (Table I) that slow heating promotes the formation of long secondary bubble rows by joining of the original primary ones, as shown in Figure 11.

Although the results of the measurements of the bubble diameters (Figure 6) provide direct evidence for the coarsened bubble structure of the slowly heated samples, on the basis of the TEM micrographs we could not make an assessment of the lengths of the bubble rows. Nevertheless, the evolution of longer primary grains in the slowly heated wire is an indirect indication of the existence of longer bubble barriers that are formed from the initially shorter primary bubble rows as they are dragged and swept together by the laterally moving fiber boundaries. If this is the case, one would expect that during slow heating, wider primary grains are formed in the wire, because fewer (but longer) bubble rows will control the grain morphology of the wire. Figure 1(c) and figure 3(b) indicate that this model is consistent with our observations. The results of previous studies /32/ also showed that the width of the primary grains in the annealed wire is related to the lateral spacing of the bubble rows, supporting the view that the wider primary grains in the slowly heated wire originate from greater lateral spacing of the bubble rows.

In principle, the decreased dispersion of the coarsened bubble structure in the slowly heated wire could reduce the recrystallization temperature. However, the opposite was observed: Table I shows that secondary recrystallization in the slowly heated samples always started at a higher temperature than that in the

Fig. 11: Replication TEM micrograph showing long "secondary" bubble row formed by joining of the shorter "primary" ones. As a result of row-row collision and subsequent bubble coalescence, relatively large bubbles can form at the contact part of the original rows.

case of rapid heating. Similar results were reported in our previous paper /19/ suggesting that this increase in the recrystallization temperature occurs because the slow heating can remove much of the stored energy and thus the driving force for grain growth decreases. In the discussion which follows we will show that this interpretation is consistent with the results of our present study.

Since the mechanical deformation creates in the wire not only a high dislocation density but also a very dense fiber boundary network, according to expression (2), the stored energy of a drawn tungsten wire consists of two energy terms. While in the early stage of the recrystallization process the contribution of the first

term to the driving force is relatively large, as the dislocation density decreases the influence of boundary energy becomes progressively more important. Figures 1-3 show that at the onset of secondary recrystallization the primary grains in the slowly heated wire are longer and wider than those in a rapidly heated sample, i.e. the wire has a coarser grain structure. This means that the slowly heated wires have less energy in them, and thus the driving force for exaggerated grain growth is relatively small (compared with the driving force in a rapidly heated sample) and results in a higher secondary recrystallization temperature.

The higher recrystallization temperature proved to be an important factor in the development of the higher aspect ratio of the secondary grains in the slowly heated wire (Figure 4b). By using EEM we observed that an increase in the recrystallization temperature markedly accelerated grain growth. Due to the enhanced grain boundary mobility at higher temperatures, very large primary recrystallized regions were rapidly consumed by the growing secondary grains (e.g. at 2300°C, the occupation of a 0.1 mm long part of the wire by a single large grain required usually less than 0.1 sec). The higher secondary recrystallization temperature associated with rapid grain growth in the slowly heated wire resulted in a large grained structure because other primary grains (potential "nuclei") that existed within the rapidly swept region were not able to begin to grow during the very short period of time. Presumably, in addition to the high grain boundary mobility, the large secondary grains are formed in the slowly heated sample, because the number of nuclei (grains that are able to grow) decreases as more and more stored energy is taken out of the wire.

Figure 8 and Figure 9 show that near the temperature at which secondary recrystallization starts, the decrease in hardness and the increase in average width of the fibers continued for about 20 minutes. Subsequently further changes could not be detected, i.e. after isothermal annealing for 20 minutes at 1800°C both hardness and fiber width reached a stationary (saturation) value. The results of these measurements may account for the observed recrystallization kinetics. Figure 7(b) shows that the continuation of the impeded secondary grain growth requires only a small increase in the temperature if it is applied within a few seconds after the recrystallization process had come to a standstill. As shown in Figure 8, during such a short time only a part of the stored deformation energy will be released and, therefore, the driving force in the unrecrystallized part of the wire is still large enough for further grain growth to occur at slightly higher temperature. However, when the grain growth process comes to a stop and the wire is further heated at the given temperature for 20 minutes or longer, the hardness reaches its minimum value reflecting that this time only a relatively low driving force is available. Therefore, in this case the arrested recrystallization can only be completed at a considerably higher temperature at which the increased mobility of the grain boundaries and local upsetting of the balance between the driving and pinning forces (by bubble coalescence) may allow secondary grain growth to proceed.

V. CONCLUSIONS

1. At the onset of secondary recrystallization, the primary grains are longer and slightly wider in a slowly heated wire. The final grain structures produced by secondary recrystallization also have a higher aspect ratio in the slowly heated wire.
2. The potassium bubble size in the slowly heated wire appears to be slightly coarser than in a rapidly heated wire.
3. If the secondary grain growth process stops and the grain structure of the wire remains in this condition for longer than approximately 10 minutes, the unrecrystallized part of the wire loses a large amount of its stored energy, as indicated by the hardness measurements reported in this study, and further grain growth is no longer possible at the given temperature. In this case, the arrested recrystallization can only be completed at a considerably higher temperature.
4. The lowest temperature at which complete secondary recrystallization in KSiAl-doped drawn tungsten wires can be achieved depends on the applied heating rate; as the heating rate decreases this temperature increases.
5. Our results are consistent with a model which

suggests that upon slow heating some bubble rows coalesce. This coalescence would allow the larger bubbles to form, which were observed in the slowly heated wire, and it could produce longer bubble rows, which could aid in the formation of the higher aspect ratio grains in the primary recrystallized structure. As the boundaries move in the slowly heated samples, they may drag the bubble rows along, which would aid in the coalescence.

ACKNOWLEDGEMENTS

The authors would like to acknowledge many helpful discussions with many people. At the General Electric Research and Development Center, they include Dr. Alan Taub and Dr. Bernard Bewlay. At GE TUNGSRAM, they include Istvan Meszaros, Csaba Toth and Dr. Attila Nagy. At the Research Institute for Technical Physics of the Hungarian Academy of Sciences, they include Dr. Laszlo Bartha and Dr. Istvan Gaal. They would also like to thank Mr. Michael Larsen of the General Electric Research and Development Center for performing the TEM and Mrs. Olga Geszti of RITP-HAS for performing the fracture replica examinations. Two of us (OH and KH) wish to thank the General Electric Research and Development Center for their assistance in this work which was partially performed while they were visiting scientists at the R&D Center, Schenectady.

REFERENCES

1. R.W. Weeks, S.R. Pati, M.F. Ashby and P. Barrand, *Acta Metall.*, 17, 1403-1410 (1969).
2. B. Burton, *Phil. Mag. A*, **43**, 1-10 (1981).
3. E. Pink and L. Bartha, *The Metallurgy of Doped/Non-Sag Tungsten*, Elsevier Sci. Publ. Ltd., London, 1989.
4. H.G. Sell, D.F. Stein, R. Stickler, A. Joshi and E. Berkei, *J. Inst. Met.*, 100, 275-288 (1972).
5. W.D. Schubert, B. Lux and B. Zeiler, *Int. J. Refractory and Hard Mat.*, **13**, 119-135 (1995).
6. B.P. Bewlay and C.L. Briant, *Int. J. Refractory and Hard Mat.*, **13**, 137-160 (1995).
7. J. Neugebauer and L. Bartha, *Int. J. Refractory and Hard Mat.*, **13**, 1-34 (1995).
8. D.M. Moon and R.C. Koo, *Metall. Trans.*, **2**, 2115-2122 (1971).
9. C.L. Briant, *Metall. Trans. A*, **24**, 1073-1084 (1993).
10. O. Horacsek, Cs. Toth, I. Gaal and K. Horacsek, *Proc. 12th Int. Plansee Sem.*, Reutte, 1, 513-521 (1989).
11. M.R. Vukcevich, *Proc. 5th Int. Tungsten Symp.*, Budapest, MPR Publishing, Shrewsbury, U.K., 1992; 157-168.
12. G.D. Rieck, *Acta Metall.*, 9, 825-832 (1961).
13. J.L. Walter, *Trans. Met. Soc. AIME*, **239**, 272-286 (1967).
14. A. Berghezan and A. Fourdeux, *Planseeber. Pulvermet.*, **22**, 264-284 (1974).
15. H. Warlimont, G. Necker and H. Schultz, *Z. Metallkd.*, **66**, 279-286 (1975).
16. D.B. Snow, *Metall. Trans.*, 7A, 783-794 (1976).
17. S. Yamazaki, S. Ogura, Y. Fukazawa and N. Hatae, *High Temp.-High Press.*, **10**, 329-339 (1978).
18. K. Tanoue, E. Masaoka and H. Matsuda, *Proc. 1st Int. Conf. on the Metallurgy and Materials Science of Tungsten, Titanium, Rare Earths and Antimony*, **2**, 730-735 (1988).
19. C.L. Briant, O. Horacsek and K. Horacsek, *Metall. Trans. A*, **24A**, 843-851 (1993).
20. O. Horacsek, *High Temperature Materials and Processes*, 14, 91-96 (1995).
21. D.B. Snow, in: *The Metallurgy of Doped/Non-Sag Tungsten*, E. Pink and L. Bartha (eds), Elsevier, Barking, England, 1989; 189-202.
22. H.H.R. Jansen, *Philips J. Res.*, **42**, 3-14 (1987).
23. C. Zener, cited by C.S. Smith in *Trans. AIME*, **175**, 15-51 (1948).
24. H.P. Stüwe, *Metall. Trans. A*, **17A**, 1455-1459 (1986).
25. O. Horacsek, *Z. Metallkd.*, **63**, 269-273 (1972).
26. B.P. Bewlay, N. Lewis and K.A. Lou, *Metall. Trans.*, **23A**, 121-133 (1992).
27. C.L. Briant, *Metall. Trans.*, **24A**, 1073-1084 (1993).

28. M.V. Speight and G.W. Greenwood, *Phil. Mag.*, 9, 683-689 (1964).
29. F.A. Nichols, *J. Am. Ceram. Soc.*, **51**, 468-469 (1968).
30. R.J. Brook, *J. Am. Ceram. Soc.*, **52**, 56-57 (1969).
31. O. Horacsek, M. Menyhárd and J. Lábár, *High Temperature Materials and Processes*, **14**, 207-213 (1995).
32. J.L. Walter and C.L. Briant, "Tungsten Wire for Incandescent Lamps", *GE CR&D 'Report* (May, 1990).